

This discussion paper is/has been under review for the journal Hydrology and Earth System Sciences (HESS). Please refer to the corresponding final paper in HESS if available.

Selecting the optimal method to calculate daily global reference potential evaporation from CFSR reanalysis data

F. C. Sperna Weiland^{1,2}, C. Tisseuil³, H. H. Dürr¹, M. Vrac⁴, and L. P. H. van Beek¹

¹Department of Physical Geography, Utrecht University, P.O. Box 80115, 3508 TC, Utrecht, The Netherlands

²Deltares, P.O. Box 177, 2600 MH, Delft, The Netherlands

³UMR BOREA-IRD 207/CNRS 7208/MNHN/UPMC, Muséum National d'Histoire Naturelle, Département Milieux et Peuplements Aquatiques, Paris, France

⁴Laboratoire des Sciences du Climat et de l'Environnement (LSCE-IPSL) CNRS/CEA/UVSQ, Centre d'étude de Saclay, Orme des Merisiers, 91191 Gif-sur-Yvette Cedex, France

Received: 1 July 2011 – Accepted: 18 July 2011 – Published: 28 July 2011

Correspondence to: F. C. Sperna Weiland (frederiek.sperna@deltares.nl)

Published by Copernicus Publications on behalf of the European Geosciences Union.

HESSD

8, 7355–7398, 2011

Selecting the optimal method to calculate daily

F. C. Sperna Weiland et al.

Title Page

Abstract

Introduction

Conclusions

References

Tables

Figures

⏪

⏩

◀

▶

Back

Close

Full Screen / Esc

Printer-friendly Version

Interactive Discussion

Abstract

Potential evaporation (PET) is one of the main inputs of hydrological models. Yet, there is limited consensus on which PET equation is most applicable in hydrological climate impact assessments. In this study six different methods to derive global scale reference PET time series from CFSR reanalysis data are compared: Penman-Monteith, Priestley-Taylor and original and modified versions of the Hargreaves and Blaney-Criddle method. The calculated PET time series are (1) evaluated against global monthly Penman-Monteith PET time series calculated from CRU data and (2) tested on their usability for modeling of global discharge cycles.

The lowest root mean squared differences and the least significant deviations (95 % significance level) between monthly CFSR derived PET time series and CRU derived PET were obtained for the cell specific modified Blaney-Criddle equation. However, results show that this modified form is likely to be unstable under changing climate conditions and less reliable for the calculation of daily time series. Although often recommended, the Penman-Monteith equation did not outperform the other methods. In arid regions (e.g., Sahara, central Australia, US deserts), the equation resulted in relatively low PET values and, consequently, led to relatively high discharge values for dry basins (e.g., Orange, Murray and Zambezi). Furthermore, the Penman-Monteith equation has a high data demand and the equation is sensitive to input data inaccuracy. Therefore, we preferred the modified form of the Hargreaves equation, which globally gave reference PET values comparable to CRU derived values. Although it is a relative efficient empirical equation, like Blaney-Criddle, the equation considers multiple spatial varying meteorological variables and consequently performs well for different climate conditions. In the modified form of the Hargreaves equation the multiplication factor is uniformly increased from 0.0023 to 0.0031 to overcome the global underestimation of CRU derived PET obtained with the original equation. It should be noted that the bias in PET is not linearly transferred to actual evapotranspiration and runoff, due to limited soil moisture availability and precipitation.

Selecting the optimal method to calculate daily

F. C. Sperna Weiland et al.

Title Page

Abstract

Introduction

Conclusions

References

Tables

Figures



Back

Close

Full Screen / Esc

Printer-friendly Version

Interactive Discussion



The resulting gridded daily PET time series provide a new reference dataset that can be used for future hydrological impact assessments or, more specifically, for the statistical downscaling of daily PET derived from raw GCM data.

1 Introduction

Climate change is likely to induce alterations in the hydrological cycle (IPCC, 2007). To assess and quantify the possible changes, multiple hydrological impact studies have been conducted on the local, continental and global scale, the latter being of interest in this study. In addition to temperature and precipitation, evapotranspiration is one of the main components of the water balance at the land surface and required as input for hydrological models used in impact studies (Kay and Davies, 2008; Oudin et al., 2005). Whereas precipitation and temperature model input data are usually at hand, actual evapotranspiration (AET; for list of abbreviations see Table 1) is seldomly monitored. Furthermore, within hydro-climatic change studies, raw General Circulation Model (GCM) data and statistically or dynamically downscaled GCM data are frequently used to force global hydrological models (Sperna Weiland et al., 2011a). Yet, these datasets often lack AET data (PCMDI, 2010). Moreover, we prefer the calculation of potential evaporation (PET) from other GCM meteorological variables and the derivation of AET with a hydrological model over using GCM AET directly. This because within GHMs, AET is calculated on a higher grid resolution and processes related to transpiration and soil moisture are schematized in more detail (Sperna Weiland et al., 2011b). In addition, AET of GCMs is often biased due to, amongst others, biases in precipitation and radiation (Mahanama and Koster, 2005; Elshamy et al., 2009). As a consequence, creating reference daily PET time-series that can be used as meteorological input for hydrological models is crucial in order to derive consistent AET, runoff and discharge (Oudin et al., 2005).

There is limited consensus on which PET equation is most applicable in global hydrological impact studies. Several studies illustrated that the selection of a method can

Selecting the optimal method to calculate daily

F. C. Sperna Weiland et al.

Title Page

Abstract

Introduction

Conclusions

References

Tables

Figures

⏪

⏩

◀

▶

Back

Close

Full Screen / Esc

Printer-friendly Version

Interactive Discussion



actually determine the direction of projected change in future water availability (Boorman, 2010; Kingston et al., 2009; Arnell, 1999). Note however, that the influence of biases and uncertainties in PET usually decreases while moving within the hydrological model chain from PET to AET to discharge, as water availability becomes limited (Vörösmarty et al., 1998).

Generally, the Penman-Monteith equation is considered as the standard (Hargreaves et al., 2003; Droogers and Allen, 2002; Gavilán et al., 2006). This equation is preferred over simpler temperature based methods in climate impact studies because it includes the effect of changes in multiple atmospheric variables (Kay and Davies, 2008; Arnell, 1999; Kingston, 2009). On the other hand, Penman-Monteith has a high input data requirement and, especially when input data is subject to inaccuracy, as is the case with reanalysis and GCM data, quality of the resulting PET might decrease (Oudin et al., 2005). Therefore the Hargreaves equation is often used as an alternative (Hargreaves and Samani, 1985; Hargreaves et al., 2003). Contrary to simpler empirical temperature based equations, like Blaney-Criddle (Blaney and Criddle, 1950), Hargreaves also considers the influence of humidity by an approximation with the diurnal temperature range. The equation is applicable in a variety of climatic conditions and no local calibration is needed. Globally, agreement between PET derived with Penman-Monteith and Hargreaves has been found to be reasonable (Droogers and Allen, 2002). Several studies tried to improve the Hargreaves equation by including aridity functions and wind data. However, the influence of these parameters on the quality of the calculated evaporation was limited (Hargreaves et al., 2003 and references therein).

There is an ongoing discussion on the reliability of the different methods, especially when working with reanalysis or GCM data. It could be questioned whether a physically based Penman-Monteith like formula with a high sensitivity to inaccuracy in input data would be more reliable than a more empirical equation with less input parameters and therefore smaller spread in uncertainties (Kingston et al., 2009). And maybe, the Priestley-Taylor equation, in which the aerodynamic term of the Penman-Monteith equation is replaced by an empirical multiplier, could better be used (Weiß and Menzel,

Selecting the optimal method to calculate daily

F. C. Sperna Weiland et al.

Title Page

Abstract

Introduction

Conclusions

References

Tables

Figures



Back

Close

Full Screen / Esc

Printer-friendly Version

Interactive Discussion



2008; Lu et al., 2005). In addition, in order to reduce the computation time required for both calculation of PET and downscaling of the required input variables, the Blaney-Criddle equation might be useful as well. The Blaney-Criddle equation is an empirical temperature-based equation and it has given results comparable to the other PET methods (Oudin et al., 2005; Blaney and Criddle, 1950). Yet, Jensen (1966) showed that the climate dependency of the empirical Blaney-Criddle equation disables its application in multiple different climate zones. To overcome this problem, Ekström et al. (2007) presented three different methods to spatially bias-correct Blaney-Criddle PET. In this study we adopt their best performing method as one of the six methods we investigate. In addition, we investigate a modification of the more physically based empirical Hargreaves equation (Droogers and Allen, 2002), which might be less sensitive to climate conditions since a larger number of spatial varying meteorological variables are considered as input.

Seeing the variety of equations which all have their pros and cons, there is still a need to properly select the PET equation to be used within hydrological modeling studies, especially at continental to global scales. This selection will depend both on the meteorological dataset and the study area of interest. For the global analysis in this study, the Climate Forecast System Reanalysis (CFSR) dataset is used (Saha et al., 2006; Saha et al., 2010) because it has a high spatial ($\sim 0.3^\circ \times \sim 0.3^\circ$ degrees) and temporal (6-hourly) resolution and it supersedes the frequently used earlier US NCEP/NCAR (National Center for Environmental Prediction/National Center for atmospheric research) reanalysis data (Kalnay et al., 1996). The dataset contains the required daily atmospheric fields to calculate and compare a range of PET equations and it can be used for the downscaling of raw GCM data to higher spatial resolution at a daily time-scale.

Daily input of PET equations increasingly becomes available and daily PET is often required as input for hydrological models. Therefore we decided to focus on calculation of daily PET time series using daily values of the required atmospheric variables instead of calculating monthly PET and downscaling this to daily values (for example based on temperature) as has frequently been done before (Sperna Weiland et al.,

Selecting the optimal method to calculate daily

F. C. Sperna Weiland et al.

Title Page

Abstract

Introduction

Conclusions

References

Tables

Figures



Back

Close

Full Screen / Esc

Printer-friendly Version

Interactive Discussion

2010; Arnell, 2011), since for a correct temporal downscaling not only air temperature is important. The diurnal temperature range, vapor pressure, and incoming shortwave radiation influence PET as well and should preferably not be neglected in a temporal downscaling procedure. Yet, considering all these variables would result in complex empirical temporal downscaling relations.

This study is a preliminary step for the assessment of future global hydrological consequences of climate change. For this assessment the global hydrological model PCR-GLOBWB will be run with downscaled GCM data. A first analysis illustrated the value of directly downscaling PET derived from raw GCM data, based on the reference PET time series created in this study. The “direct” downscaling approach was preferred over downscaling of the individual GCM input variables of the PET equation, since in independent procedures inconsistencies between the atmospheric input variables of the PET equations can be introduced (Piani et al., 2010). For future downscaling, PET will first be calculated from raw GCM data at the original GCM resolution. In a second step, the GCM derived PET will be downscaled with the here created reference CFJR PET time series, hereby generating bias-corrected GCM PET time series at the resolution of the hydrological model.

The main goal of this study is the construction of a global gridded dataset of reference PET at high spatial (0.5 degree) and temporal (daily) resolution from CFJR reanalysis data. Not only should the constructed PET dataset show high resemblance with the measurement based monthly PET time-series derived from the CRU datasets which are often considered as a standard (New et al., 2000, 1999, Droogers and Allen, 2002; IPCC, 2007), the dataset should also be a reliable reference for the statistical downscaling of daily PET time series calculated from raw GCM data, which can be used as input for hydrological climate impact studies.

We will first compare six PET equations for the creation of daily PET time series; Penman-Monteith, Hargreaves, Priestley-Taylor, Blaney-Criddle and modifications of the Hargreaves and Blaney-Criddle equation. All equations are applied to the CFJR reanalysis dataset for the period 1979–2002 and the resulting PET time series are

HESSD

8, 7355–7398, 2011

Selecting the optimal method to calculate daily

F. C. Sperna Weiland et al.

Title Page

Abstract

Introduction

Conclusions

References

Tables

Figures



Back

Close

Full Screen / Esc

Printer-friendly Version

Interactive Discussion



evaluated against Penman-Monteith PET derived from the CRU datasets (New et al., 2000, 1999). In a second step, the transfer of bias in PET to modeled AET, runoff and discharge is assessed by inter-method comparison and comparison of modeled river discharge with discharge observations.

2 Data and methods

2.1 CFSR reanalysis data

The CFSR dataset is a reanalysis product which is developed as part of the Climate Forecast System (Saha et al., 2006, 2010) at the National Centers for Environmental Prediction (NCEP). The CFSR dataset became available in 2010 and supersedes the previous NCEP/NCAR reanalysis dataset which has been widely used in downscaling studies (e.g. Michelangeli et al., 2009; Maurer et al., 2010; Wilby et al., 2002). At this stage the CFSR dataset spans the period 1979 to present and has a resolution of approximately 0.25 degrees around the equator to 0.5 degrees beyond the tropics (Higgins et al., 2010). In this study, 6-hourly temperature, radiation, air pressure and wind data were averaged to a daily time-step for the period 1979–2002. These daily time series were then interpolated to a regular 0.5 degrees grid (using bilinear interpolation) in order to calculate PET at the grid resolution of the global water balance model PCR-GLOBWB.

2.2 CRU reference potential evaporation

For validation reference historical PET time series were calculated from the CRU datasets with the FAO recommended Penman-Monteith equation (Monteith, 1965; Allen et al., 1998). Temperature, vapor pressure, diffusivity and net incoming radiation were retrieved from the CRU TS2.1 monthly time series (New et al., 2000). Cloud cover and wind speed were obtained from the monthly climatology, CRU CLIM 1.0

Selecting the optimal method to calculate daily

F. C. Sperna Weiland et al.

Title Page

Abstract

Introduction

Conclusions

References

Tables

Figures



Back

Close

Full Screen / Esc

Printer-friendly Version

Interactive Discussion



(New et al., 1999) because monthly CRU TS2.1 time series are not provided for these variables.

2.3 Potential evaporation equations

Within this study, daily PET time series derived from six different PET equations were compared. The equations ranged from the physically based Penman-Monteith (PM) equation, to the radiation- and temperature-based Hargreaves (HG) and Priestley-Taylor (PT) equations, to the simple temperature-based Blaney-Criddle (BC) equation and additional modified forms of the Hargreaves and Blaney-Criddle equation (Table 2).

The BC equation was applied in its original form (BCorig) and in a re-calibrated form (BCrecal) following Ekström et al. (2007). In this modified BC equation, the multiplicative and additive coefficients (e.g., 0.46 and 8) have been re-calibrated to cell-specific values (see the resulting coefficient values in Fig. 1). This was done by linearly regressing the cell specific long-term average mean monthly CFSR temperature to the CRU derived long-term average monthly PET for the complete period with overlapping data available for the two datasets (1979–2002). The slopes and intercepts of this linear regression exercise were used to calculate the coefficient values. For the empirical BC equation, which considers only limited meteorological variables, a cell specific re-calibration was preferred (this is also illustrated by the large spatial variation in bias between BC PET derived from CFSR data and reference PM PET derived from CRU data, as will be presented in the results section).

A simpler globally uniform modification was applied to the HG equation following Allen (1993) and Droogers and Allen (2002). The Hargreaves equation is an efficient empirical equation with low input data demand. Yet, the equation considers spatial variation in climate conditions in more detail as it also includes the daily temperature range and spatial radiation pattern. PET derived from the CFSR dataset with the original HG (HGorig) equation underestimates CRU PET with a small spatial variability, as will be shown in the results section. To increase the HG PET globally, we increased the multiplication factor for all grid cells uniformly from 0.0023 to 0.0031 by linear fitting long

Selecting the optimal method to calculate daily

F. C. Sperna Weiland et al.

Title Page

Abstract

Introduction

Conclusions

References

Tables

Figures

⏪

⏩

◀

▶

Back

Close

Full Screen / Esc

Printer-friendly Version

Interactive Discussion



term average monthly HG PET against long term average monthly CRU PET (HGrecal). To this end, the multiplication factor was varied with intervals of 0.0001 until the lowest global average RMSD value was obtained for the monthly average PET time series.

2.4 Global hydrological modelling

The global water balance was modelled with the global hydrological model PCR-GLOBWB. For a detailed description and validation of the model, see Van Beek et al. (2011), Van Beek and Bierkens (2009) and Sperna Weiland et al. (2010). Each model cell, with a resolution of 0.5 degrees, consists of two vertical soil layers and one underlying groundwater reservoir. Sub-grid parameterization is used for the schematization of surface water, short and tall vegetation and for calculation of saturated areas for surface runoff as well as interflow. Water enters the cell as rainfall and can be stored as canopy interception or snow. Snow is accumulated when temperature is below 0°C and melts when temperature is higher. Melt water and throughfall are passed to the surface, where they either infiltrate in the soil or become surface runoff. Exchange of soil water is possible between the soil and groundwater layers in both up- and downward direction, depending on soil moisture status and groundwater storage. Total runoff consists of non-infiltrating melt water, saturation excess surface runoff, interflow and base flow.

Within the hydrological model, AET is derived from PET time series. The total AET flux exists of plant transpiration and bare soil evaporation, which spatially depend on the presence of crop types and soil moisture conditions. Within the model in a first step, reference PET is transferred to crop specific and bare soil PET values by multiplication with the minimum crop factor (for bare soil) or with the monthly climatology of crop factors (Van Beek, 2008) which have been projected on the 0.5 degrees hydrological model grid for the specific crop types:

$$ES_o = k_s PET \quad (1)$$

Selecting the optimal method to calculate daily

F. C. Sperna Weiland et al.

Title Page

Abstract

Introduction

Conclusions

References

Tables

Figures

⏪

⏩

◀

▶

Back

Close

Full Screen / Esc

Printer-friendly Version

Interactive Discussion



$$T_o = k_c \text{PET} \quad (2)$$

where PET is reference PET (m day^{-1}), k_s is the “crop factor” used for bare soil, ES_0 is potential bare soil evaporation (m day^{-1}), k_c is the monthly crop factor and T_o is potential crop specific transpiration (m day^{-1}).

Reduction of potential bare soil evaporation and potential plant transpiration to AET depends on soil moisture storage. For the saturated fraction of the soil no reduction occurs, except that the rate of potential evaporation can not exceed the saturated hydraulic conductivity. Potential bare soil evaporation of the un-saturated fraction is limited by the un-saturated hydraulic conductivity. Transpiration only occurs for the un-saturated fraction of the soil and depends on the total available soil moisture storage in the models soil layers (Van Beek, 2008).

For each daily time step the water balance, and its resulting runoff and AET fluxes, are computed for all model cells. The cell specific runoff is accumulated and routed as river discharge along the drainage network taken from the global Drainage Direction Map (DDM30; Döll and Lehner 2002) using the kinematic wave approximation of the Saint-Venant equation.

2.5 Statistical validation

The six PET time series derived from CFRS data were validated for the period 1979 to 2002 against monthly CRU based Penman-Monteith PET time series (CRUPM) and compared with each other, using six statistical quantities:

1. global maps of biases in long-term average annual means:

$$\text{BIAS} = \overline{\text{PET}}_{\text{CFRSR}} - \overline{\text{PET}}_{\text{CRU}} \quad (3)$$

where $\overline{\text{PET}}_{\text{CFRSR}}$ refers to annual average PET calculated from the CFRS dataset using one of the six equations (Table 2) and $\overline{\text{PET}}_{\text{CRU}}$ refers to the annual average PET calculated from the CRU dataset with the Penman-Monteith equation.

Selecting the optimal method to calculate daily

F. C. Sperna Weiland et al.

Title Page

Abstract

Introduction

Conclusions

References

Tables

Figures

⏪

⏩

◀

▶

Back

Close

Full Screen / Esc

Printer-friendly Version

Interactive Discussion



Selecting the optimal method to calculate daily

F. C. Sperna Weiland et al.

Title Page

Abstract

Introduction

Conclusions

References

Tables

Figures

⏪

⏩

◀

▶

Back

Close

Full Screen / Esc

Printer-friendly Version

Interactive Discussion

2. global maps of areas with significant differences between CRU and CFSR derived PET, AET, runoff and discharge. These maps indicate for all six methods for all hydrological quantities of interest (PET, AET, local runoff and discharge) whether the CFSR derived values deviate significantly from the CRU derived values. The map comparison is restricted to deviations between results of PCR-GLOBWB runs forced with the full CFSR dataset (i.e. CFSR precipitation (PR), temperature (TAS) and PET calculate with one of the six equations) and the PCR-GLOBWB run forced with the full CRU dataset downscaled to daily values with the CFSR dataset. For the evaluation of differences in station discharge, results of PCR-GLOBWB runs forced with CRU PR and TAS and CFSR PET have been included as well, this in order to exclude the influence of biases in CFSR PR from the analysis. Significance of differences between CRU and CFSR PET derived values has been quantified with the Welch's t-test for a significance level of 95 %.

$$t = \frac{\bar{X}_{\text{CRU}} - \bar{X}_{\text{CFSR}}}{\sqrt{\frac{s_{\text{CRU}}^2}{n_{\text{CRU}}} + \frac{s_{\text{CFSR}}^2}{n_{\text{CFSR}}}}} \quad (4)$$

Where \bar{X}_{CRU} is the average value calculated from the CRU dataset and \bar{X}_{CFSR} is the long term annual average calculated from the CFSR dataset for one of the six equations, S_{CRU} is the standard deviation of the 24 CRU derived annual values and S_{CFSR} is the standard deviation of the 24 CFSR derived values, n_{CFSR} and n_{CRU} are the numbers (24) of annual average values for both datasets.

3. global maps of cell specific root mean squared differences (RMSD; m day^{-1}) of the monthly time series (Eq. 5) have been created. These maps give an indication of regional performance on the smallest time-scale at which validation data is

provided:

$$\text{RMSD} = \sqrt{\frac{\sum_{i=1}^N (\text{PET}_{\text{CRU}_i} - \text{PET}_{\text{CFSR}_i})^2}{N}} \quad (5)$$

where PET_{CFSR} refers to the monthly PET calculated from the CFSR data set, PET_{CRU} refers to the monthly PM-based PET calculated from the CRU dataset, i is the month number and N is the total number of months ($N = 288$).

4. for each season individually, the mean (Eq. 6) of the global cell specific seasonal RMSD values (as in Eq. (5), except for monthly values being replaced by seasonal values) quantifies the overall performance of the PET methods and the standard deviation (Eq. 7) quantifies the spatial variability in performance:

$$\overline{\text{RMSD}} = \frac{\sum_{j=1}^M \text{RMSD}_j}{M} \quad (6)$$

$$\text{SDV}_{\text{RMSD}} = \sqrt{\frac{\sum_{j=1}^M (\text{RMSD}_j - \overline{\text{RMSD}})^2}{M}} \quad (7)$$

where $\overline{\text{RMSD}}$ (m day^{-1}) is the mean of all cell specific seasonal RMSD values (RMSD_j), j is the grid cell number, M is the total number of grid cells and SDV_{RMSD} (m day^{-1}) is the standard deviation of all cell specific seasonal RMSD values.

5. global maps with long-term average and seasonal average PET, AET and runoff have been calculated to illustrate the differences between methods. Biases

Selecting the optimal method to calculate daily

F. C. Sperna Weiland et al.

Title Page

Abstract

Introduction

Conclusions

References

Tables

Figures

⏪

⏩

◀

▶

Back

Close

Full Screen / Esc

Printer-friendly Version

Interactive Discussion



Selecting the optimal method to calculate daily

F. C. Sperna Weiland et al.

Title Page	
Abstract	Introduction
Conclusions	References
Tables	Figures
⏪	⏩
◀	▶
Back	Close
Full Screen / Esc	
Printer-friendly Version	
Interactive Discussion	

Discussion Paper | Discussion Paper | Discussion Paper | Discussion Paper | Discussion Paper | Discussion Paper | Discussion Paper | Discussion Paper | Discussion Paper | Discussion Paper

distributions shown in dark grey (hereafter called full CRU run; for the temporal downscaling procedure see Sperna Weiland et al. (2010)). (3) Discharge calculated with a PCR-GLOBWB run forced with a combination of CFSR derived PET and temporally downscaled CRU PR and TAS, hereby the influence of possible PR biases present in the CFSR dataset have been minimized. The results of these runs are shown by the group of bars on the right for each river. (4) Finally, for validation of all modeled discharge values, observed discharge obtained from the GRDC (GRDC, 2007) is modified by adding an estimation of water use (Wada et al., 2010; Sperna Weiland et al., 2010) the resulting corrected discharge is included in the charts in black.

3 Results

3.1 Global reference potential evaporation

3.1.1 Long-term average bias

The biases in long-term average CFSR annual PET from CRU PM PET show large differences for the six PET equations (Fig. 2). Penman-Monteith PET derived from CFSR data (CFSRPM) underestimates Penman-Monteith PET derived from CRU data (CRUPM) in arid regions (e.g. the Sahara, Central Australia and the southwest of the US) and slightly overestimates CRUPM in southeast Asian Islands and parts of the Amazon basin (Fig. 2a). The Priestley-Taylor equation (CFSRPT) highly overestimates CRUPM in the Amazon basin, Central Africa and Indonesia, whereas underestimations similar to those of the CFSRPM are present in the Sahara and parts of Australia (Fig. 2d). The standard Hargreaves equation (CFSRHGorig) underestimates CRUPM globally (Fig. 2b). By increasing the multiplication factor of the HG equation from 0.0023 to 0.0031, the lowest global average RMSD was obtained (Fig. 2e). Similar increases of this coefficient have also been proposed by Droogers and Allen



(2002) and Allen (1993). PET calculated with the Blaney-Criddle equation (CFSRBC) is too high for almost the entire world (Fig. 2c). Overestimations are especially large in Central Africa and Central South-America. Yet, PET calculated with the re-calibrated Blaney-Criddle equation from the CFSR dataset (CFSRBCrecal) results in the highest similarity with CRUPM (Fig. 2f). For illustrational purpose, global maps of absolute PET values for the different methods are shown in the Supplement (Fig. A).

3.1.2 RMSD of monthly time series

The lowest monthly RMSD values are obtained for the BCrecal equation and the HGrecal equation (Fig. 3e and f). The pattern of RMSD values of PM and PT (Fig. 3a and d) are comparable, although the RMSD is slightly higher for CFSRPT over the Amazon basin and Central-Africa. The similarity of PET derived from the two equations is caused by the radiation term present in both equations. Overall, the global maps in Fig. 3 show that performance of the PT, HGorig and BCorig equations is low, whereas the HGrecal equation and especially the BCrecal equation perform well.

3.1.3 Significance of differences

In Fig. 4 the significance of differences between the annual average PET, AET and local runoff derived from CFSR data (with any of the PET equations) and annual average values of the same variables derived from CRU data is indicated. Within Fig. 4 black areas correspond to regions where annual averages of CFSR and CRU PET derived values are similar. Large regions with CFSR PET values similar to CRU PET only occur for the BCcal method. The BCorig and HGorig equations obviously show least significant resemblance with CRU PET. While moving from PET to AET to local runoff (QL) the areas with similar CRU and CFSR derived annual average values increase in size. Note as well that the differences, in areas with significant deviations, between the different PET methods decrease due to both limited soil moisture availability and the influence of PR on local runoff and discharge.

Selecting the optimal method to calculate daily

F. C. Sperna Weiland et al.

Title Page

Abstract

Introduction

Conclusions

References

Tables

Figures



Back

Close

Full Screen / Esc

Printer-friendly Version

Interactive Discussion



3.1.4 Global mean seasonal RMSD

The global mean and standard deviation of the cell specific RMSD values of seasonal PET, derived from the difference between CRUPM and the different CFSR PET time series (Eq. 5), have been calculated for the individual seasons to quantify the global seasonal performance and its spatial variability (Fig. 5). For all four seasons the BCrecal equation gave the lowest global average RMSD values and the HGrecal equation performed second best (Fig. 5). This confirms the performance improvement obtained by re-calibration of the two equations on long-term average monthly means of temperature and evaporation. The BCrecal method performs best, which could be expected after cell-specific re-calibration. Yet, due to the large spatial variability of the coefficient values (Fig. 1), the stability of the equation under changing climate conditions is not guaranteed. In addition, the daily BCrecal PET values span a relatively small range. The extreme daily values are modest compared to daily PET values derived with the other equations (for brevity, the full analysis has not been included, but as an example cumulative distribution functions (CDFs) of daily PET values are given for the MacKenzie, Amazon, Rhine and Zambezi river basins in Fig. 6). This may be a result of the use of the equation on a daily time scale instead of the monthly time scale for which the equation was originally designed.

For the DJF, MAM and SON seasons, RMSD values of the PM, PT and BC methods are comparable. However, performance of the original BC equation is especially poor for the JJA season (Northern hemisphere boreal summer), the season in which evaporation has the largest influence on the water balance. For all seasons, except JJA, highest RMSD values are obtained with the HGorig equation.

The standard deviation of the cell specific RMSD values is an indication of the spatial variability in performance (Fig. 5, error bars). The highest standard deviations are obtained from the PM and PT equation. The standard deviation of the HGorig equation is slightly lower, indicating a more constant performance in space. Increasing the multiplication factor in the HGorig equation to 0.0031 (HGrecal) did not only result in

Selecting the optimal method to calculate daily

F. C. Sperna Weiland et al.

Title Page

Abstract

Introduction

Conclusions

References

Tables

Figures



Back

Close

Full Screen / Esc

Printer-friendly Version

Interactive Discussion

a lower global mean RMSD, but also decreased the spatial variability in performance. The highest spatially consistent performance was obtained for the BCrecal equation.

3.2 Impact of different PET equations on actual evapotranspiration and runoff

For the evaluation of CFSR PET, global PET time series derived from CRU data with the PM equation, could be used as a reference. Unfortunately, there are no reference global gridded time series of AET available for the evaluation of the impact of the different PET equations on modeled discharge. Vörösmarty et al. (1998) apply an approximation of observed AET by subtracting observed runoff from observed PR. Yet, within in the study of Vörösmarty et al. (1998) it is already stated that this approximation is only valid in areas with little water regulation or abstractions and reliable PR and discharge measurements. As was also the case for several locations in their study, we obtained negative AET values for a number of basins and concluded that the method was not reliable when being used in combination with our global datasets. Therefore, the CFSR derived AET and runoff maps are not explicitly validated. Here, only a comparison between methods is made. In Sect. 3.3 the bias in AET is evaluated by comparison of the resulting modeled discharge with observed GRDC discharge. Although illustrative it should be noted that this comparison might be flawed by discharge measurement and hydrological model errors.

3.2.1 Variation between methods

Biases in CFSR PET from CRU PET are reduced while moving from PET to AET and runoff since AET is limited by soil moisture conditions. Consequently AET biases, are lower than biases in PET. Limitation by soil moisture deficits mainly occurs in arid regions (e.g., the Sahara, Central Australia and the South-Western US) or in the dry seasons. Global maps with annual average AET and runoff show the impact of deviations in PET on AET and runoff (Fig. 7.1 and 7.2). Globally the variability between the six different methods is smaller for AET than for PET, as can be seen from the cell specific

Selecting the optimal method to calculate daily

F. C. Sperna Weiland et al.

Title Page

Abstract

Introduction

Conclusions

References

Tables

Figures

⏪

⏩

◀

▶

Back

Close

Full Screen / Esc

Printer-friendly Version

Interactive Discussion



values for the coefficient of variation (CV) obtained from the PET values calculated for the six different methods (Fig. 8). The global cell average coefficient of variation (CV) for PET is 0.42, whereas for AET and runoff the CV values are respectively 0.25 and 0.27. High CV values for PET and AET are obtained for Northern regions and the Himalayas. Yet, CV values for runoff are low in these regions due to the relatively low absolute amount of AET related to the low air temperature and the large influence of PR. High CV values for PET are also present in the Sahara and central Australia as a result of the large underestimations of CRUPM PET in these regions by CFSRPT and CFSRPM PET. However, soil moisture is limited in these dry regions and AET amounts are comparably low for the different methods resulting in low CV values.

Over South-East Asia, the Eastern US, parts of Europe, Russia and the Amazon and Congo basins, high CV values of 0.2 to 0.3 are obtained for both PET and AET. Here, except for South-East Asia, where there is a strong influence of the Monsoon precipitation, AET amounts are high and, the high CV values for AET are translated to high CV values for runoff. Only for those regions where both the CV of runoff generated by the different PET is high and the absolute runoff amounts are of significant value, the selected PET method is likely to have a large impact on modeled runoff and discharge amounts.

3.2.2 Comparison of actual evapotranspiration

Absolute AET is relatively high for CFSRPM for the Amazon and Congo basins and the islands of southeast-Asia (Fig. 7.1a). For these regions, even higher AET values are obtained with the PT and BCorig equations (Fig. 7.2a and c), resulting in low runoff values. AET calculated from both BCorig and BCrecal PET is high in Northern Europe and the Eastern US especially in the JJA season (Fig. 7.1c and 7.2c). This results in slightly lower runoff values for these regions (Fig. 7.1f). The lowest AET values are derived from HGorig PET (Fig. 7.2b) and even AET derived from HGrecal is relatively low. High similarity in AET values is found for HGrecal and BCrecal (Fig. 7.1b and

Selecting the optimal method to calculate daily

F. C. Sperna Weiland et al.

Title Page

Abstract

Introduction

Conclusions

References

Tables

Figures

⏪

⏩

◀

▶

Back

Close

Full Screen / Esc

Printer-friendly Version

Interactive Discussion



c). For illustrative purposes global maps of seasonal AET values are given in the Supplement (Fig. B).

3.2.3 Comparison of runoff

Figures 4, 7.1 and 7.2 show that differences in spatial runoff patterns are almost as small as the differences in AET patterns. This is a result of the fact that the runoff flux is influenced by both evapotranspiration and precipitation. Runoff is low for the PT and BCorig method (Fig. 7.2d and f). Although increasing the multiplication factor in the original HG equation to 0.0031 resulted in higher PET values, the difference in runoff derived from the two HG equations is still small (Fig. 7.1e and 7.2e). Global seasonal runoff maps for the different PET equation are provided as Supplement (Fig. C).

3.3 Impact of different PET equations on discharge

The PET time series created in this study will be used in further research to downscale daily PET time series derived from raw GCM data. The downscaled PET time series can be employed for global hydrological impact assessments. We used the global hydrological model PCR-GLOBWB to evaluate the influence of the different PET equations on AET and river discharge. The model was forced with the daily CFSR PET time series, and both the CFSR and CRU PR and TAS, in subsequent steps. The latter was done to assess the influence of the bias in precipitation on modeled discharge as well.

3.3.1 Variation between methods

While being illustrative, the differences in runoff obtained from the six methods are hard to distinguish from the global runoff maps (Fig. 7.1, 7.2 and 4). Therefore, basin specific discharge CV values, calculated from the discharges modeled with PCR-GLOBWB using the different CFSR PET time series as input, are listed in Table 3 for 19 large rivers at measurement stations close to the catchment outlets. Basin discharge CV values are even lower than CV values for runoff, due to accumulation of processes

Selecting the optimal method to calculate daily

F. C. Sperna Weiland et al.

Title Page

Abstract

Introduction

Conclusions

References

Tables

Figures

⏪

⏩

◀

▶

Back

Close

Full Screen / Esc

Printer-friendly Version

Interactive Discussion



along the river network. CV values of river discharge (QC) range between 0.05 and 0.34 and are on average 0.20. This indicates that the selection of a PET method is of minor relevance for modeled discharge (Oudin et al., 2005). The smallest variations in discharge between the different PET methods are found in the Monsoon influenced catchments where precipitation dominates discharge patterns. High CV values (0.26–0.30) are obtained for the Zambezi, Murray and Orange, basins in dry climate where PET has a large influence on resulting discharge. High values are also obtained for the Amazon (0.28) and Congo (0.34). In these tropical basins, the high variability between PET methods, results in high variability in runoff and discharge as well, due to the humid climate. Contrary to the results of Oudin et al. (2005) this illustrates that for those basins with high CV values, which are unavoidable part of global scale studies, the selection of a PET equation does influence modeled discharge.

3.3.2 Deviations from observed discharge

Discharge calculated from the different PET equations and either CFSR or CRU PR and TAS are compared with observed discharge and discharge derived from CRU PET in Fig. 9. The charts show that discharge derived from CFSR PET calculated with the BCorig equation is the lowest for all basins and underestimates corrected observed discharge for 6 out of 19 basins for both the runs forced with CFSR PR as well as for the runs forced with temporally downscaled CRU PR. Relatively low values are also obtained with the BCreval and especially the PT equation. Discharges calculated from HGorig PET are highest for all basins.

In an overall comparison of the full CFSR runs with the corrected GRDC discharge and results of the full CRU run, BCorig performs the best. Discharge modeled from CFSR PET derived with this method has the lowest percentage bias from corrected GRDC discharge for 11 out of 19 basins and the lowest percentage bias from the full CRU run for 5 out of 19 basins. The BCreval method performs second best (lowest bias from corrected GRDC and full CRU run for 4 out of 19 basins). The HGorig method also shows good performance (best for 2 out of 19 in comparison with corrected GRDC and

Selecting the optimal method to calculate daily

F. C. Sperna Weiland et al.

Title Page

Abstract

Introduction

Conclusions

References

Tables

Figures



Back

Close

Full Screen / Esc

Printer-friendly Version

Interactive Discussion



best for 5 out of 19 in comparison with full CRU run). However, as mentioned above, the HGorig discharge is the highest for all basins and the BCorig discharge is the lowest for all basins. These results suggest that these two methods perform the best for wrong reasons. The extreme values are likely to compensate for biases in observed discharge (McMillan et al., 2010; Vrugt et al., 2005) and biases in precipitation (Fekete et al., 2004; Biemans et al., 2009).

The influence of using either CFSR PR or CRU PR can be analyzed from Fig. 9 by comparing the group of bars on the left and right side for each river. For example for the Amazon, Parana, Orange and Niger the use of CRU PR amounts results in much higher discharges, whereas for the Mekong, MacKenzie, Lena and Indus, CRU PR results in lower discharges. Differences between annual average discharge obtained from the two precipitation products are especially small for the Rhine, Murray and Yellow river.

Additional PCR-GLOBWB runs have been executed based on CFSR derived PET time series and the measurement based CRU PR and TAS (bars on the right). This in order to minimize the influence of precipitation bias on modeled discharge and to distinguish the bias originating from PET from the bias originating from precipitation. The run based on CFSR HGrecal PET performs best for 11 out of 19 in comparison with the full CRU run, and best for 3 out of 19 in comparison with corrected GRDC discharge. In comparison with corrected GRDC discharge, the BCreval (best for 7 basins) and BCorig (best for 8 basins) methods perform better. Yet, the BCorig method, which results in the lowest discharge values, mainly performs best for the dry basins (e.g. the Murray, Orange, Zambezi and Niger) where the hydrological model tends to underestimate AET and consequently overestimates discharge (Van Beek et al., 2011).

In Sect. 3.2.1 the impact of differences between ETP methods on resulting river discharge was quantified with CV values. Within the bar charts in Fig. 9 the differences in runoff are displayed as well. Again it can be seen that for some basins the difference in discharge obtained from the different PET methods is large, see for example the Amazon and Congo, where due to the humid climate reduction from PET to AET is small. The difference is also large for the Mississippi which course travels through multiple

Selecting the optimal method to calculate daily

F. C. Sperna Weiland et al.

Title Page	
Abstract	Introduction
Conclusions	References
Tables	Figures
⏪	⏩
◀	▶
Back	Close
Full Screen / Esc	
Printer-friendly Version	
Interactive Discussion	



climate zones (e.g. from sub-Arctic to semi-arid) and river discharge is therefore affected by differences in PET in at least part of the basin. Differences between methods are small for; (1) the Niger and Orange due to limiting soil moisture conditions, (2) the Lena because, as a result of the low temperatures, absolute AET amounts are low for this basins and (3) the Indus where river discharge is highly influenced by precipitation.

3.3.3 Significance in deviations from CRU derived discharge

In Fig. 10a and b the significance of the differences between annual average (station) discharge (QC) derived from CRU and CFSR PET is indicated for PCR-GLOBWB runs forced with both full CFSR forcing and the forcing dataset existing of CFSR PET and CRU PR and TAS. Green squares correspond to similar annual average discharge derived from CFSR and CRU PET, red squares indicate significant differences for a level of 95 %.

Notable is the difference between QC derived from the full CFSR forcing and QC derived from CFSR PET and CRU PR and TAS amounts. When PCR-GLOBWB is forced with the observation based CRU PR and TAS and CFSR PET, significant differences from CRU PET derived values occur most often for the BCorig and HGorig equations. While for PCR-GLOBWB runs forced with the full CFSR dataset, the four other equations show lowest similarity with QC derived from CFSR PET. This indicates that the PET time series compensate for difference between CRU and CFSR PR. When evaluating the performance of the different PET equations for model runs forced with the observation based CRU PR and TAS, the BCrecal equation shows highest similarity with full CRU derived QC and the PT, PM and HGrecal equations also perform well.

4 Discussion and conclusions

In this study six different methods, to globally derive daily PET time series from CFSR reanalysis data, have been evaluated on (1) their resemblance with monthly PET time

Selecting the optimal method to calculate daily

F. C. Sperna Weiland et al.

Title Page

Abstract

Introduction

Conclusions

References

Tables

Figures



Back

Close

Full Screen / Esc

Printer-friendly Version

Interactive Discussion



5 calculation of monthly instead of daily time series (Blaney and Criddle, 1950). Yet, in this study we violated this assumption and used the equation to calculate daily values, which are required as input to the hydrological model PCR-GLOBWB. As a consequence the daily BC_{recal} PET spanned a relatively small range of daily PET values compared to the other methods (Fig. 6). Secondly, discharge derived from BC_{recal} PET is too low compared to the other methods for most basins (second lowest after BC_{orig} derived runoff or lowest for 12 out of 19 basins, Fig. 9). Finally, the values of the Blaney-Criddle coefficients show a high spatial variability (Fig. 1) due to the cell specific re-calibration which was required because of the large spatial variation in bias of CFSR BC PET from CRU PET. The sensitivity of the coefficients to the spatially varying climate conditions (Jensen, 1966) suggests that they will also be sensitive to future changing climate conditions. By contrast, the Hargreaves equation, which could be globally uniform re-calibrated due to its small spatial variation in bias, performs well in multiple climate zones and is therefore also likely to perform well under changing climate conditions. It is also an efficient empirical equation, yet more spatial varying meteorological variables are considered than in the Blaney-Criddle equation, which increases its possibilities for spatial transfer. The large adjustment of the multiplication factor from 0.0023 to 0.0031 significantly improves the goodness-of-fit of the Hargreaves equation, similar increases were also suggested by Droogers and Allen (2002). The adjustment may directly result from the application of the equation to a daily time-step while the equation is said to perform best over longer time-steps (10 days-month; Hargreaves, 2003). From the discussion above we conclude that, for the calculation of daily PET time series from CFSR reanalysis data, the re-calibrated HG equation is the most reliable equation.

25 **Supplementary material related to this article is available online at:**
<http://www.hydrol-earth-syst-sci-discuss.net/8/7355/2011/hessd-8-7355-2011-supplement.pdf>

Selecting the optimal method to calculate dailyF. C. Sperna Weiland et al.

Title Page

Abstract

Introduction

Conclusions

References

Tables

Figures

⏪

⏩

◀

▶

Back

Close

Full Screen / Esc

Printer-friendly Version

Interactive Discussion



Acknowledgements. The global discharge time series have been obtained from the Global Runoff Data Centre. The CFSR reanalysis products used in this study are obtained from the Research Data Archive (RDA) which is maintained by the Computational and Information Systems Laboratory (CISL) at the National Center for Atmospheric Research (NCAR). NCAR is sponsored by the National Science Foundation (NSF). The original data are available from the RDA (<http://dss.ucar.edu>) in dataset number ds093.0. H. H. Dürr, was partly funded by the EU FP6 program “Carbo-North”(contract nr. 036993).

References

- Allen, R. G., Pereira, L. S., Raes, D., and Smith M.: Crop evapotranspiration: FAO Irrigation and drainage paper 56, FAO, Rome, Italy, 1998.
- Allen, R. G.: Evaluation of a temperature difference method for computing grass reference evapotranspiration. Report submitted to the Water Resources Development and Man Service, Land and Water Development Division, FAO, Rome, 49 pp., 1993.
- Arnell, N. W.: Uncertainty in the relationship between climate forcing and hydrological response in UK catchments, *Hydrol. Earth Syst. Sci.*, 15, 897–912, doi:10.5194/hess-15-897-2011, 2011.
- Arnell, N. W.: The effect of climate change on hydrological regimes in Europe: a continental perspective, *Global Environ. Chang.*, 9, 5–23, 1999.
- Biemans, H., Hutjes, R. W. A., Kabat, P., Strengers, B., Gerten, D., and Rost, S.: Effects of precipitation uncertainty on discharge calculations for main river basins, *J. Hydrometeorol.*, 10(4), 1011–1025, doi:10.1175/2008JHM1067.1, 2009.
- Blaney, H. F. and Criddle, W. P.: Determining water requirements in irrigated areas from climatological and irrigation data, USDA (SCS) TP-96, 48, 1950.
- Boorman, H.: Sensitivity analysis of 18 different potential evapotranspiration models to observed climatic change at German climate stations, *Climatic Change*, 104(3–4), 729–753, doi:10.1007/s10584-010-9869-7, 2010.
- Droogers, P. and Allen, R. G.: Estimating reference evapotranspiration under inaccurate data conditions, *Irrig. Drain. Syst.*, 16, 33–45, 2002.
- Eckström, M., Jones, P. D., Fowler, H. J., Lenderink, G., Buishand, T. A., and Conway, D.: Regional climate model data used within the SWURVE project – 1: projected changes

Selecting the optimal method to calculate daily

F. C. Sperna Weiland et al.

Title Page

Abstract

Introduction

Conclusions

References

Tables

Figures



Back

Close

Full Screen / Esc

Printer-friendly Version

Interactive Discussion



Selecting the optimal method to calculate daily

F. C. Sperna Weiland et al.

Title Page

Abstract

Introduction

Conclusions

References

Tables

Figures

⏪

⏩

◀

▶

Back

Close

Full Screen / Esc

Printer-friendly Version

Interactive Discussion

in seasonal patterns and estimation of PET, *Hydrol. Earth Syst. Sci.*, 11, 1069–1083, doi:10.5194/hess-11-1069-2007, 2007.

Elshamy, M. E., Seierstad, I. A., and Sorteberg, A.: Impacts of climate change on Blue Nile flows using bias-corrected GCM scenarios, *Hydrol. Earth Syst. Sci.*, 13, 551–565, doi:10.5194/hess-13-551-2009, 2009.

Fekete, B. M., Vörösmarty, C. J., Roads, J. O., and Willmott, C. J.: Uncertainties in precipitation and their impacts on runoff estimates, *J. Clim.*, 17, 294–304, 2004.

Gavilan, P., Lorite, I. J., Tornero, S., and Berengena, J.: Regional calibration of Hargreaves equation for estimating reference ET in a semiarid environment, *Agr. Water Manag.*, 81, 257–281, doi:10.1016/j.ag.wat.2005.05.001, 2006

Hargreaves, G. H. and Samani, Z. A.: Reference crop evapotranspiration from temperature, *Appl. Eng. Agric.*, 1(2), 96–99, 1985.

Hargreaves, G. H., Asce, F., and Allen, R. G.: History and evaluation of Hargreaves evapotranspiration equation, *J. Irrig. Drain. E.-ASCE*, 129(1), 53–63, 2003.

Higgins, R. W., Kousky, V. E., Silva, V. B. S., Becker, E., and Xie, P.: Intercomparison of Daily Precipitation Statistics over the United States in Observations and in NCEP Reanalysis Products, *J. Climate*, 23, 4637–4650, doi:10.1175/2010JCLI3638.1, 2010.

IPCC: Climate change 2007: Synthesis report – summary for policy makers, 2007.

Jensen, M. E.: Discussion of “irrigation water requirements of lawns.”, *J. Irrig. Drain. Div.*, 92, 95–100, 1966.

Kalnay, E., Kanamitsu, M., Kistler, R., Collins, W., Deaven, D., Gandin, L., Iredell, M., Saha, S., White, G., Woollen, J., Zhu, Y., Leetmaa, A., Reynolds, R., Chelliah, M., Ebisuzaki, W., Higgins, W., Janowiak, J., Mo, K.C., Ropelewski, C., Wang, J., Jenne, R., and Joseph, D.: The NCEP/NCAR 40-year reanalysis project, *Bull. Amer. Meteor. Soc.*, 77, 437–470, 1996.

Kay, A. L. and Davies, V. A.: Calculating potential evaporation from climate model data: A source of uncertainty for hydrological climate change impacts, *J. Hydrol.*, 358, 221–239, doi:10.1016/j.jhydrol.2008.06.005, 2008.

Kingston, D. G., Todd, M. C., Taylor, R. G., and Thompson, J. R.: Uncertainty in the estimation of potential evapotranspiration under climate change, *Geophys. Res. Lett.*, 36, L20403, doi:10.1029/2009GL040267, 2009.

Lu, J., Sun, G., McNulty, S. G., and Amatya, D. M.: A comparison of six potential evapotranspiration methods for regional use in the southeastern united states, *J. Am. water res. As.*, 41(2), 621–633, 2005.

Selecting the optimal method to calculate daily

F. C. Sperna Weiland et al.

Title Page

Abstract

Introduction

Conclusions

References

Tables

Figures

⏪

⏩

◀

▶

Back

Close

Full Screen / Esc

Printer-friendly Version

Interactive Discussion



Mahanama, S. P. P. and Koster, R. D.: AGCM biases in evaporation regime: Impacts on soil moisture memory and land-atmosphere feedback, *J. Hydrometeor.*, 6, 656–669, doi:10.1175/JHM446.1, 2005.

Maurer, E. P., Hidalgo, H. G., Das, T., Dettinger, M. D., and Cayan, D. R.: The utility of daily large-scale climate data in the assessment of climate change impacts on daily streamflow in California, *Hydrol. Earth Syst. Sci.*, 14, 1125–1138, doi:10.5194/hess-14-1125-2010, 2010.

McMillan, H., Freer, J., Pappenberger, F., Krueger, T., and Clark, M.: Impacts of uncertain river flow data on rainfall-runoff model calibration and discharge predictions, *Hydrol. Process.*, 24, 1270–1284, 2010.

Michelangeli, P.-A., Vrac, M., and Loukos, H.: Probabilistic downscaling approaches: application to wind cumulative distribution functions, *Geophys. Res. Lett.*, 36, L11708, doi:10.1029/2009GL038401, 2009.

Monteith, J. L.: Evaporation and environment, *Symp. Soc. Exp. Biol.*, 19, 205–234, 1965.

New, M., Hulme, M., and Jones, P.: Representing Twentieth-Century space-time climate variability. Part 1: Development of a 1961–90 mean monthly terrestrial climatology, *J. Climate*, 12(2), 829–856, 1999.

New, M., Hulme, M., and Jones, P.: Representing Twentieth-Century Space–Time Climate Variability. Part II: Development of 1901–96 Monthly Grids of Terrestrial Surface Climate, *J. Climate*, 13(13), 2217–2238, 2000.

Oudin, L., Hervieu, F., Michel, C., Perrin, C., Andréassian, V., Anctil, F., and Loumagne, C.: Which potential evapotranspiration input for a lumped rainfall-runoff model?, Part2 – Towards a simple and efficient potential evapotranspiration model for rainfall-runoff modelling, *J. Hydrol.*, 303, 290–306, doi:10.1016/j.jhydrol.2004.08.026, 2005.

PCMDI: Program for Climate Model Diagnosis and Intercomparison data portal, <https://esg.llnl.gov:8443/index.jsp>, 2010.

Piani, C., Weedon, G. P., Best, M., Gomes, S. M., Viterbo, P., Hagemann, S., and J. O., Haerter: Statistical bias correction of global simulated daily precipitation and temperature for the application of hydrological models, *J. Hydrol.*, 395(3–4), 19–9–215, doi:10.1016/j.jhydrol.2010.10.024, 2010.

Priestley, C. H. B. and Taylor, R. J.: On the assessment of surface heat flux and evaporation using large-scale parameters. *Mon. Weather Rev.*, 100(1), 81–92, 1972.

Saha, S., Nadiga, S., Thiaw, C., Wang, J., Wang, W., Zhang, Q., Van den Dool, H. M., Pan, H.-L., Moorthi, S., Behringer, D., Stokes, D., Peña, M., Lord, S., White, G., Ebisuzaki, W., Peng,

Selecting the optimal method to calculate daily

F. C. Sperna Weiland et al.

Title Page

Abstract

Introduction

Conclusions

References

Tables

Figures

⏪

⏩

◀

▶

Back

Close

Full Screen / Esc

Printer-friendly Version

Interactive Discussion



- P., and Xie, P.: The NCEP Climate Forecast System, *J. Climate*, 19, 3483–3517, 2006.
- Saha, S., Moorthi, S., Pan, H.-L., Wu, X., Wang, J., Nadigam S., Tripp, P., Kistler, R., Wooll, J., Behringer, D., Lu, H., Stokes, D., Grumbine, R., Gayno, G., Wang, J., Hou, Y.-T., Chuang, H.-Y., Juang, H.-M. H., Sela, J., Iredell, M., Treadon, R., Kleist, D., Van Delst, P., Keyser, D., Derber, J., Ek, M., Meng, J., Wei, H., Yang, R., Lord, S., Van den Dool, H., Kumar, A., Wang, W., Long, C., Chelliah, M., Xue, Y., Huang, B., Schemm, J.-K., Ebisuzaki, W., Lin, R., Xie, P., Chen, M., Zhou, S., Higgins, W., Zou, C.-Z., Liu, Q., Chen, Y., Han, Y., Cucurull, L., Reynolds, R. W., Rutledge, G., and Goldberg, M.: The NCEP Climate Forecast System Reanalysis, *Bull. Amer. Meteorol. Soc.*, 1015–1057, 2010.
- Sperna Weiland, F. C., van Beek, L. P. H., Kwadijk, J. C. J., and Bierkens, M. F. P.: The ability of a GCM-forced hydrological model to reproduce global discharge variability, *Hydrol. Earth Syst. Sci.*, 14, 1595–1621, doi:10.5194/hess-14-1595-2010, 2010.
- Sperna Weiland, F. C., van Beek, L. P. H., Kwadijk, J. C. J., and Bierkens, M. F. P.: Global patterns of change in runoff regimes for 2100, *Climatic Change*, submitted, 2011a.
- Sperna Weiland, F. C., van Beek, L. P. H., Kwadijk, J. C. J., and Bierkens, M. F. P.: On the suitability of GCM runoff fields for river discharge modeling; a case study using model output from HadGEM2 and ECHAM5, *J. Hydrometeorol.*, in press, 2011b.
- Van Beek, L. P. H., Wada, Y., and Bierkens, M. F. P.: Global monthly water stress: I. Water balance and water availability, *Water Resour. Res.*, in press, doi:10.1029/2010WR009791, 2011.
- Vörösmarty, C. J., Federer, C. A., and Schloss, A. L.: Potential evaporation functions compared on US watersheds: Possible implications for global-scale water balance and terrestrial ecosystem modeling, *J. Hydrol.*, 207, 147–169, 1998.
- Vrugt, J. A., Diks, C. G. H., Gupta, H. V., Bouten, W., and Verstraten, J. M.: Improved treatment of uncertainty in hydrologic modeling: Combining the strengths of global optimization and data assimilation, *Water Resour. Res.*, 41, W01017, doi:10.1029/2004WR003059, 2005.
- Wada, Y., Van Beek, L. P. H., Van Kempen, C. M., Reckman, J. W. T. M., Vasak, S., and Bierkens, M. F. P.: Global depletion of groundwater resources, *Geophys. Res. Lett.*, 37, L20402, doi:10.1029/2010GL044571, 2010.
- Weiß, M. and Menzel, L.: A global comparison of four potential evapotranspiration equations and their relevance to stream flow modelling in semi-arid environments, *Adv. Geosci.*, 18, 15–23, <http://www.adv-geosci.net/18/15/2008/>, 2008.
- Wilby, R. L., Wigley, T. M. L., Conway, D., Jones, P. D., Hewitson, B. C., Main, J., and Wilks,

D. S.: Statistical downscaling of general circulation model output: A comparison of methods, *Water Resour. Res.*, 34(11), 2995–3008, 1998.
Wilby, R. L., Dawson, C. W., and Barrow, E. M.: SDSM – a decision support tool for the assessment of regional climate change impacts, *Environ. Modell. Softw.*, 17, 145–157, 2002.

HESSD

8, 7355–7398, 2011

Selecting the optimal method to calculate daily

F. C. Sperna Weiland et al.

Title Page

Abstract

Introduction

Conclusions

References

Tables

Figures



Back

Close

Full Screen / Esc

Printer-friendly Version

Interactive Discussion

Table 1. List of abbreviations.

Abbreviaton	Long name/description
AET	Actual evaporation
BC	Blaney-Criddle
BCorig	Original Blaney-Criddle equation
BCrecal	Re-calibrated Blaney-Criddle equation
CDF	Cumulative distribution function
CFSR	Climate forecast system reanalysis
CFSR PET	Potential evaporation calculated from CFSR data
CFSR PM PET	Penman-Monteith potential evaporation from CFSR data
CRU	Climate research unit, University of East Anglia
CRU TS 2.1	1901–96 Monthly Grids of Terrestrial Surface Climate, CRU
CRU CLM 1.0	1961–90 mean monthly terrestrial climatology, CRU
CRU PET	Potential evaporation calculated from CRU data
CRU PM PET	Penman-Monteith potential evaporation from CRU data
CV	Coefficient of variation
DJF	December, January, February
FAO	United Nations Food and Agriculture Organization
GCM	General circulation model/global climate model
GHM	Global hydrological model
GRDC	Global runoff data centre
HG	Hargreaves equation
HGorig	Original Hargreaves equation
HGrecal	Re-calibrated Hargreaves equation
HGPET	Hargreaves potential evaporation
JJA	June, July, August
MAM	March, April, May
NCAR	National Center for Atmospheric Research
NCEP	National Centre for Environmental Prediction
PCR-GLOBWB	PCRaster code global water balance model
PET	Potential evaporation
PM	Penman-Monteith
PR	Precipitation
PT	Priestley-Taylor
QC	(Channel) discharge
QL	Cell specific runoff
RMSD	Root mean squared difference
SON	September, October, November
TAS	Temperature
US	United States

Selecting the optimal method to calculate daily

F. C. Sperna Weiland et al.

[Title Page](#)

[Abstract](#)

[Introduction](#)

[Conclusions](#)

[References](#)

[Tables](#)

[Figures](#)

[⏪](#)

[⏩](#)

[◀](#)

[▶](#)

[Back](#)

[Close](#)

[Full Screen / Esc](#)

[Printer-friendly Version](#)

[Interactive Discussion](#)



Selecting the optimal method to calculate daily

F. C. Sperna Weiland et al.

Title Page

Abstract Introduction

Conclusions References

Tables Figures

◀ ▶

◀ ▶

Back Close

Full Screen / Esc

Printer-friendly Version

Interactive Discussion

Table 2. Potential evaporation equations.

Method	Acronym	Equation	Reference
Penman-Monteith	PM	$ET_o = \frac{\Delta(R_n - G) + \rho_a c_p \frac{(e_s - e_a)}{r_a}}{\lambda_v \Delta + \gamma(1 + \frac{r_s}{r_a})}$	Monteith (1965)
Hargreaves	HGorig	$ET_o = 0.0023 \cdot R_a \cdot (\bar{T} + 17.8) \cdot TR^{0.50}$	Hargreaves and Samani (1985)
Modified Hargreaves	HGrecal	$ET_o = 0.0031 \cdot R_a \cdot (\bar{T} + 17.8) \cdot TR^{0.50}$	This study
Priestley-Taylor	PT	$ET_o = \alpha \frac{\Delta R_n}{\lambda_v(\Delta + \gamma)}$	Priestley and Taylor (1972)
Blaney-Criddle	BCorig	$ET_o = p(0.46\bar{T} + 8)$	Blaney and Criddle (1950)
recalibrated Blaney-Criddle	BCrecal	$ET_o = p(a\bar{T} + b)$	Ekström et al. (2007)

λ_v = Latent heat of vaporization ($J g^{-1}$), Δ = the slope of the saturation vapour pressure temperature relationship ($Pa K^{-1}$), R_n = Net radiation ($W m^{-2}$), G = Soil heat flux ($W m^{-2}$), c_p = specific heat of the air ($J kg^{-1} K^{-1}$), ρ_a = mean air density at constant pressure ($kg m^{-3}$), $e_s - e_a$ = vapor pressure deficit (Pa), r_s = surface resistances ($m s^{-1}$), r_a = aerodynamic resistances ($m s^{-1}$), γ = Psychrometric constant ($66 Pa K^{-1}$), R_a = extraterrestrial radiation ($MJ m^{-2} day^{-1}$), \bar{T} = mean daily temperature ($^{\circ}C$), TR = temperature range ($^{\circ}C$), α = empirical multiplier ($-; 1.26$), p = mean daily percentage of annual daytime hours (%), a and b are the coefficients of the Blaney-Criddle equation which are adjusted to cell specific values in the recalibration.

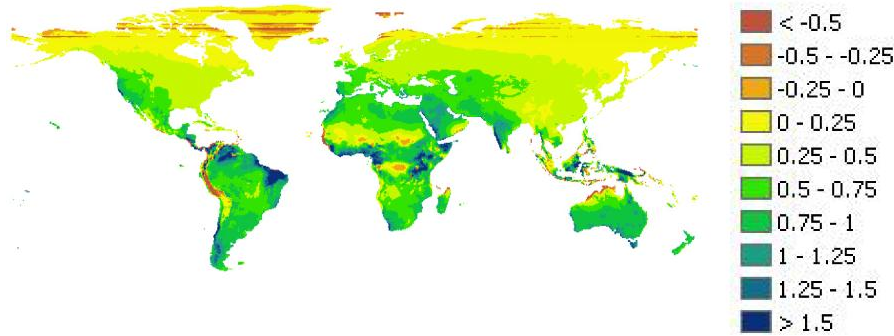
Selecting the optimal method to calculate daily

F. C. Sperna Weiland et al.

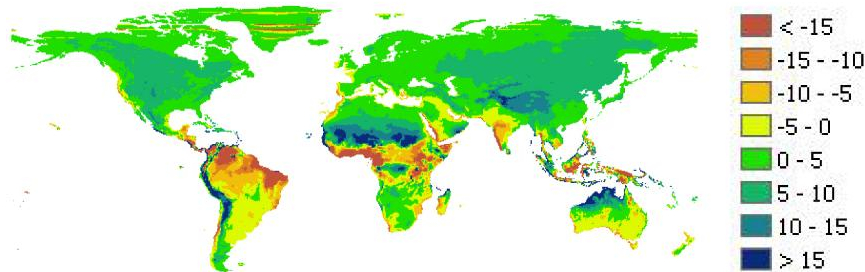
Table 3. Catchment specific coefficients of variation (CV) derived from long-term annual average modeled discharge for measurement stations closest to the catchment outlets, obtained with PET time series calculated with the six different potential evaporation equations.

Catchment	CV (–)	Catchment	CV (–)
Amazon	0.28	Murray	0.26
Brahmaputra	0.10	Niger	0.18
Congo	0.34	Orange	0.29
Danube	0.19	Parana	0.25
Ganges	0.12	Rhine	0.17
Indus	0.05	Volga	0.28
Lena	0.10	Yangtze	0.19
Mackenzie	0.24	Yellow	0.17
Mekong	0.16	Zambezi	0.30
Mississippi	0.31		

[Title Page](#)
[Abstract](#)
[Introduction](#)
[Conclusions](#)
[References](#)
[Tables](#)
[Figures](#)
[Back](#)
[Close](#)
[Full Screen / Esc](#)
[Printer-friendly Version](#)
[Interactive Discussion](#)

a.



b.

Fig. 1. Cell specific values of the coefficients in the re-calibrated Blaney-Criddle equation. The values in (a) replace the number 0.46 and the values in (b) replace the number 8 in the original Blaney-Criddle equation ($ET_o = \rho(0.46\bar{T} + 8)$).

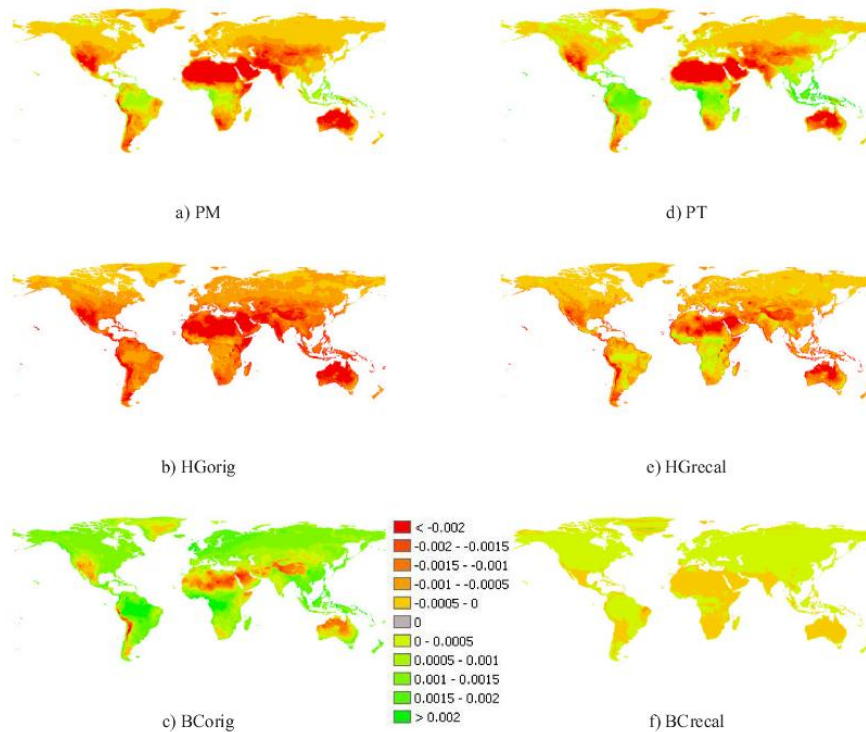


Fig. 2. Global maps with annual average bias of CFSR estimated daily reference potential evaporation (PET; m day^{-1}) from annual average CRU Penman-Monteith reference PET. In the left column bias in PET obtained with the Penman-Monteith (PM), the standard Hargreaves (HGorig) and Blaney-Cridde (BCorig) method are displayed. In the right column bias obtained with Priestley-Taylor (PT), Hargreaves with increased multiplication factor (HGrecal) and the re-calibrated Blaney-Cridde equation (BCrecal) are displayed.

Selecting the optimal method to calculate daily

F. C. Sperna Weiland et al.

Title Page

Abstract Introduction

Conclusions References

Tables Figures

⏪ ⏩

◀ ▶

Back Close

Full Screen / Esc

Printer-friendly Version

Interactive Discussion



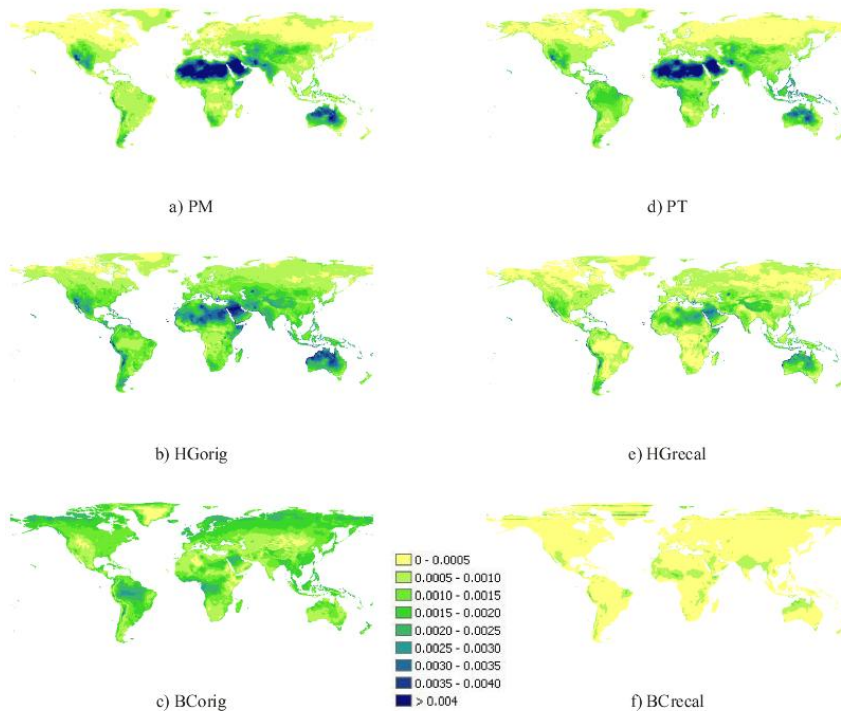


Fig. 3. Global maps with cell specific root mean square differences (RMSD) calculated between the CFSR derived monthly PET time series and the monthly PET timeseries derived from the CRU dataset with the Penman-Monteith equation. In the left column from top to bottom Penman-Monteith (PM), the original Hargreaves method (HGorig) and Blaney-Criddle equation (BCorig) and in the right column Priestley-Taylor (PT), Hargreaves with increased multiplication factor (HGrecal) and the re-calibrated Blaney-Criddle equation (BCrecal) are displayed.

Selecting the optimal method to calculate daily

F. C. Sperna Weiland et al.

Title Page

Abstract Introduction

Conclusions References

Tables Figures

⏪ ⏩

◀ ▶

Back Close

Full Screen / Esc

Printer-friendly Version

Interactive Discussion



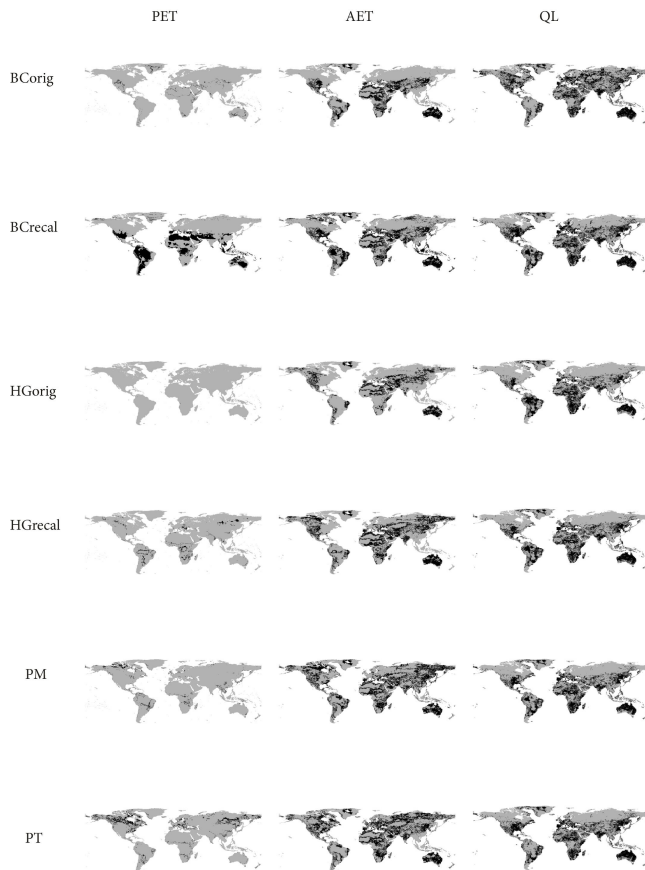


Fig. 4. Maps showing areas where CFSR derived PET, AET and local runoff (QL) significantly deviate from CRU derived values (in grey) and areas where annual average values are similar (in black) for all six PET equations.

Selecting the optimal method to calculate daily

F. C. Sperna Weiland et al.

Title Page

Abstract Introduction

Conclusions References

Tables Figures

⏪ ⏩

◀ ▶

Back Close

Full Screen / Esc

Printer-friendly Version

Interactive Discussion

Selecting the optimal method to calculate daily

F. C. Sperna Weiland et al.

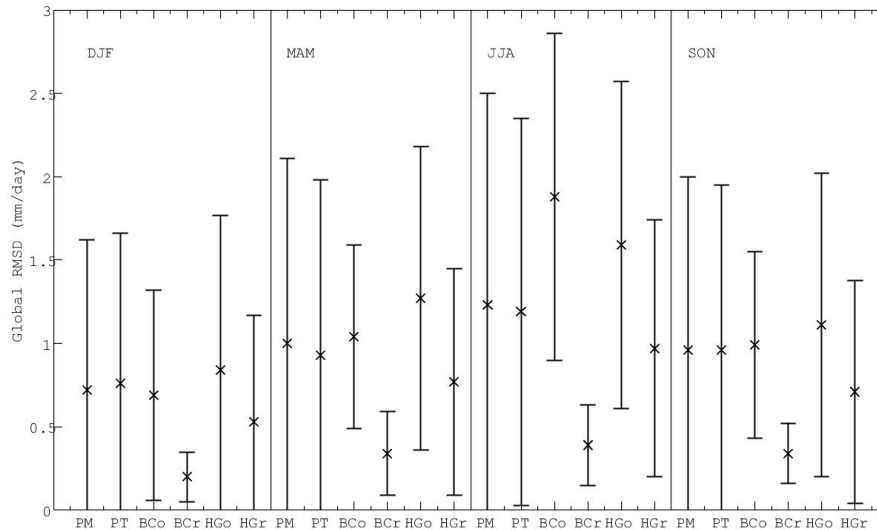


Fig. 5. Error plots with mean (crosses) and standard deviation (horizontal bars) of cell specific RMSD values (mm day^{-1}) calculated for the four seasons individually from the differences between the CFSR derived seasonal potential evaporation values and the CRU based seasonal potential evaporation. Abbreviations have been used for BCoorig (BCo), BCreval (BCr), HGoorig (HGo) and HGreval (HGr).

[Title Page](#)
[Abstract](#)
[Introduction](#)
[Conclusions](#)
[References](#)
[Tables](#)
[Figures](#)
[⏪](#)
[⏩](#)
[◀](#)
[▶](#)
[Back](#)
[Close](#)
[Full Screen / Esc](#)
[Printer-friendly Version](#)
[Interactive Discussion](#)

Selecting the optimal method to calculate daily

F. C. Sperna Weiland et al.

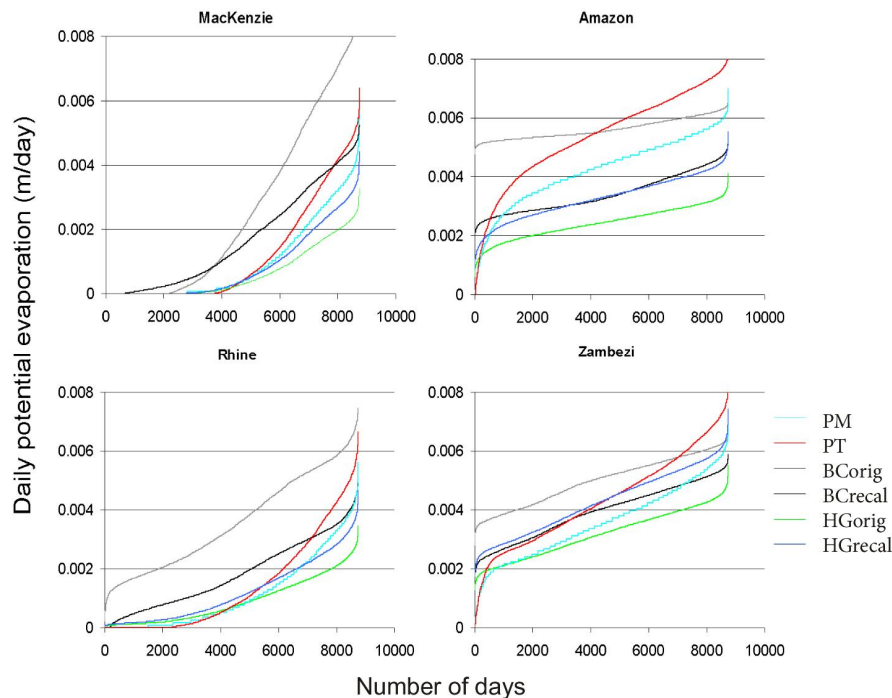


Fig. 6. CDFs of daily potential evaporation (m day^{-1}) for a selection of catchments; MacKenzie, Amazon, Rhine and Zambezi.

Title Page

Abstract Introduction

Conclusions References

Tables Figures

⏪ ⏩

◀ ▶

Back Close

Full Screen / Esc

Printer-friendly Version

Interactive Discussion



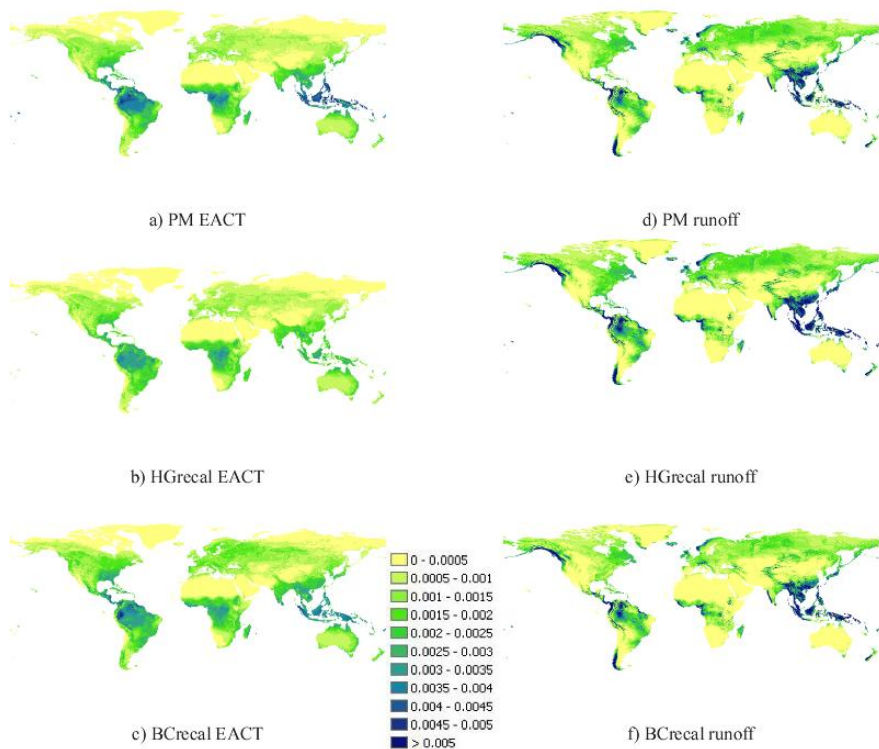


Fig. 7.1. Global maps with on the left annual average daily actual evapotranspiration (m day^{-1}) and on the right annual average daily runoff (m day^{-1}). From top to bottom, Penman-Monteith (PM), Hargreaves with increased multiplication factor (HGrecal) and re-calibrated Blaney-Criddle (BCrecal).

Selecting the optimal method to calculate daily

F. C. Sperna Weiland et al.

Title Page

Abstract Introduction

Conclusions References

Tables Figures

⏪ ⏩

◀ ▶

Back Close

Full Screen / Esc

Printer-friendly Version

Interactive Discussion



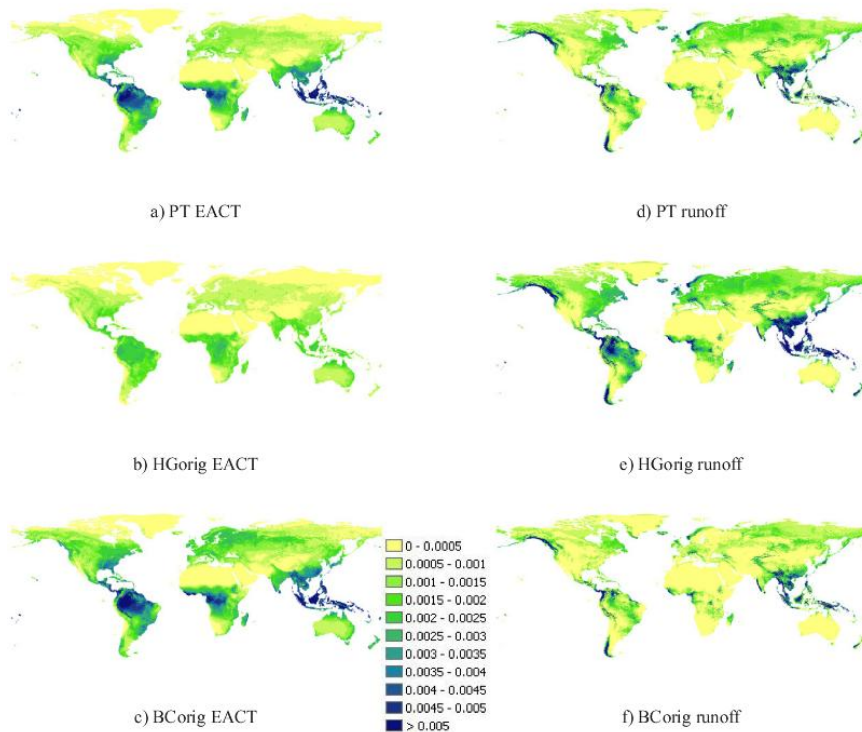


Fig. 7.2. Global maps with on the left annual average daily actual evapotranspiration (m day^{-1}) and on the right annual average daily runoff (m day^{-1}). From top to bottom, Priestley-Taylor (PT), the original Hargreaves equation (HGorig) and the original Blaney-Criddle equation (BCorig).

Selecting the optimal method to calculate daily

F. C. Sperna Weiland et al.

Title Page

Abstract Introduction

Conclusions References

Tables Figures

⏪ ⏩

◀ ▶

Back Close

Full Screen / Esc

Printer-friendly Version

Interactive Discussion



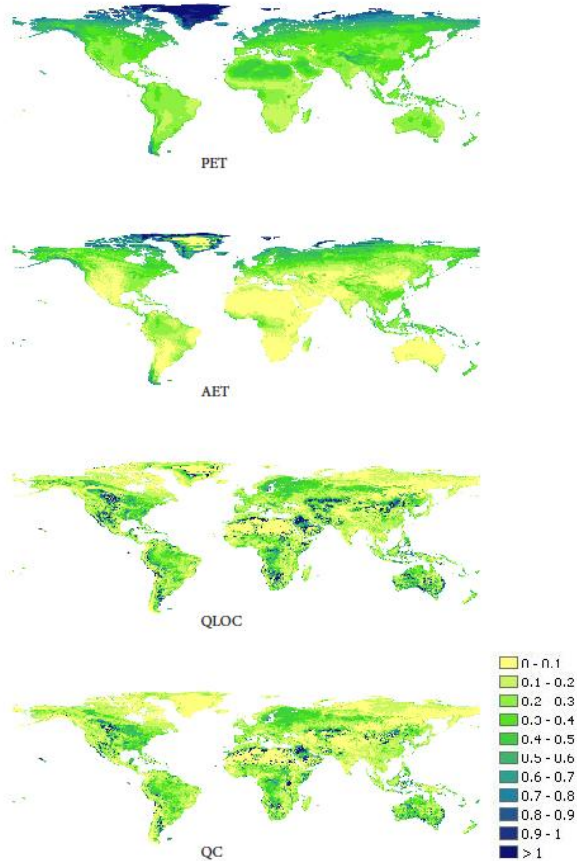


Fig. 8. Cell specific values of the coefficient of variation (CV; –) calculated from the six different potential evaporation methods for potential evaporation (PET), actual evapotranspiration (AET), local runoff (QLOC) and discharge (QC).

Selecting the optimal method to calculate daily

F. C. Sperna Weiland et al.

Title Page

Abstract Introduction

Conclusions References

Tables Figures

⏪ ⏩

◀ ▶

Back Close

Full Screen / Esc

Printer-friendly Version

Interactive Discussion



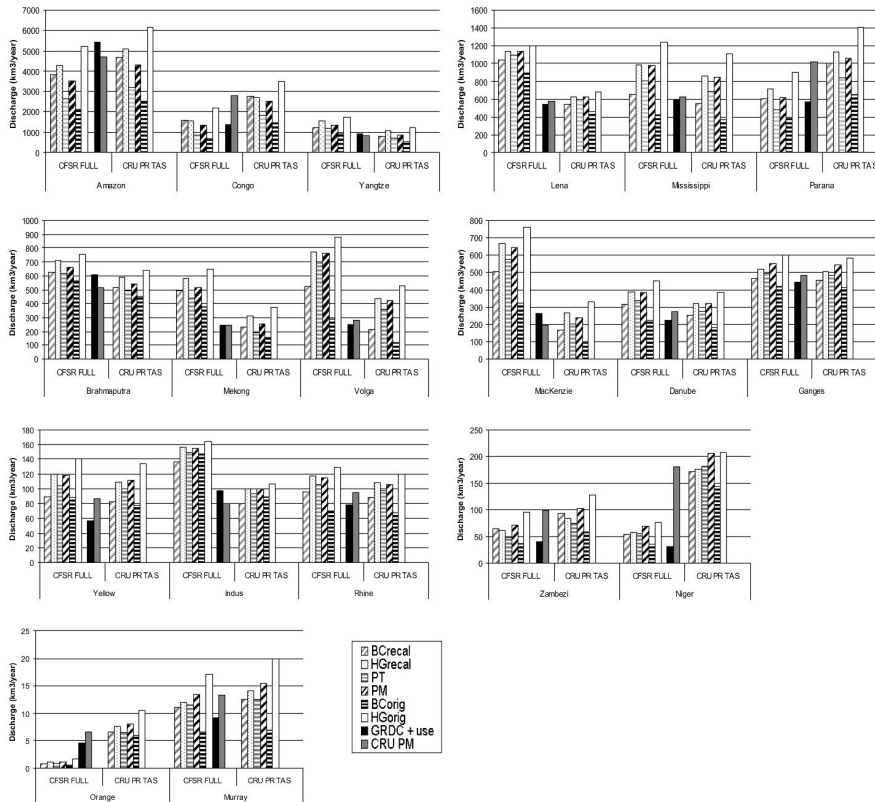


Fig. 9. Long-term average annual basin discharge ($\text{km}^3 \text{yr}^{-1}$) for 19 large river basins derived with PCR-GLOB-WB forced with PET calculated from the CFSR dataset with the six different methods (group of bars on the right for each river). As references corrected observed GRDC basin discharge (black), PCR-GLOBWB discharge modeled from the CRU dataset (dark grey) and discharges calculated from CRU precipitation, CRU temperature and CFSR PET (group of bars on the right) have been added.

Selecting the optimal method to calculate daily

F. C. Sperna Weiland et al.

Title Page

Abstract Introduction

Conclusions References

Tables Figures

◀ ▶

◀ ▶

Back Close

Full Screen / Esc

Printer-friendly Version

Interactive Discussion



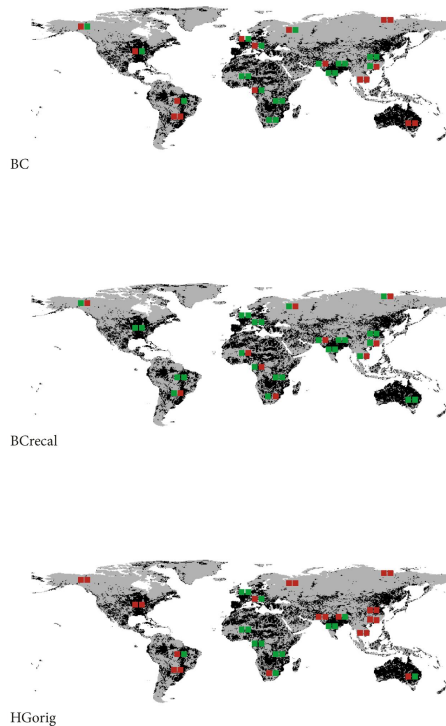


Fig. 10a. Maps showing areas where CFSR derived (station) discharge (QC) significantly deviates from CRU derived values. Grey areas correspond to cells where CFSR derived QC significantly deviates from CRU derived QC, black cells indicate areas where annual average QC is similar. Squares indicate significance of difference in station discharge for the 19 major river basins in Fig. 9 (red is significant difference, green is similar annual average values). For each river, the left square corresponds to the PCR-GLOBWB run forced with CFSR PET and CRU PR and TAS and the right square corresponds to the runs with full CFSR forcing. Statistics are given for the original and re-calibrated Blaney-Criddle equation and the original Hargreaves equation.

Selecting the optimal method to calculate daily

F. C. Sperna Weiland et al.

Title Page

Abstract Introduction

Conclusions References

Tables Figures

⏪ ⏩

◀ ▶

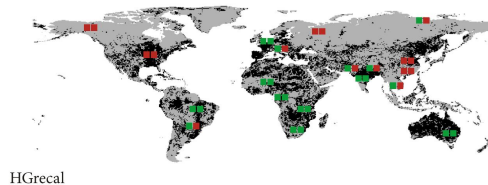
Back Close

Full Screen / Esc

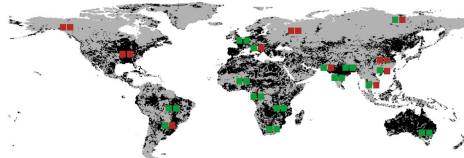
Printer-friendly Version

Interactive Discussion

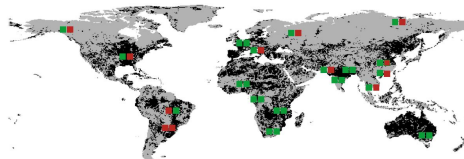




HGrecal



PM



PT

Fig. 10b. Similar to 10a, but now for the re-calibrated Hargreaves, Penman-Monteith and Priestley-Taylor equations.

Selecting the optimal method to calculate daily

F. C. Sperna Weiland et al.

Title Page

Abstract

Introduction

Conclusions

References

Tables

Figures

⏪

⏩

◀

▶

Back

Close

Full Screen / Esc

Printer-friendly Version

Interactive Discussion